

ACTINIDE BIOCOLLOID FORMATION IN BRINE BY HALOPHILIC BACTERIA

J.B. Gillow*, A.J. Francis*, C.J. Dodge*, R. Harris**, T.J. Beveridge**, P.V. Brady***,
H.W. Papenguth***

* Brookhaven National Laboratory, Upton, NY 11973, gillow@bnl.gov

** University of Guelph, Guelph, Ontario N1G 2W1, Canada

***Sandia National Laboratories, Albuquerque, NM 87185

RECEIVED

AUG 11 1999

OSTI

ABSTRACT

We examined the ability of a halophilic bacterium (WIPP 1A) isolated from the Waste Isolation Pilot Plant (WIPP) site to accumulate uranium in order to determine the potential for biocolloid facilitated actinide transport. The bacterial cell surface functional groups involved in the complexation of the actinide were determined by titration. Uranium, added as uranyl nitrate, was removed from solution at pH 5 by cells but at pH 7 and 9 very little uranium was removed due to its limited solubility. Although present as soluble species, uranyl citrate at pH 5, 7, and 9, and uranyl carbonate at pH 9 were not removed by the bacterium because they were not bioavailable due to their neutral or negative charge. Addition of uranyl EDTA to brine at pH 5, 7, and 9 resulted in the immediate precipitation of U. Transmission electron microscopy (TEM) and energy dispersive X-ray spectroscopy (EDS) analysis revealed that uranium was not only associated with the cell surface but also accumulated intracellularly as uranium-enriched granules. Extended X-ray absorption fine structure (EXAFS) analysis of the bacterial cells indicated the bulk sample contained more than one uranium phase. Nevertheless these results show the potential for the formation of actinide bearing bacterial biocolloids that are strictly regulated by the speciation and bioavailability of the actinide.

INTRODUCTION

The Waste Isolation Pilot Plant (WIPP) repository located in Southeastern New Mexico is specifically designed for the long-term isolation of transuranic (TRU) waste from the accessible environment. The effectiveness of WIPP relies on its ability to limit the migration of actinides, predominantly Pu, Am, Np, and U, in the subsurface bedded salt environment. Potential migration mechanisms include transport as soluble species or as colloids, which are generally defined as particles $< 1 \mu\text{m}$ suspended in a liquid. Actinide-bearing colloids that may be generated in the repository include mineral fragments, products from corrosion of the steel waste containers, intrinsic colloids (hydrolysis and condensation of actinide ions), and organic colloids (products from the biodegradation of cellulosic material, humic and fulvic acids, and microbial cells). The concentration of naturally occurring microbes in the hypersaline environments at WIPP is about 10^4 to 10^7 cells ml^{-1} and have exceeded 10^8 cells ml^{-1} in a simulated cellulose-rich repository environment [1, 2]. Because bacterial cells fall within the colloidal size range, typically on the order of 0.5 to 1.0 μm in length [2], and can be mobile in the subsurface, the potential for biocolloid facilitated transport of actinides under WIPP repository conditions is being investigated.

Bacterial cell walls possess a variety of negatively charged functional groups (COO^- , PO_4^{3-} , OH^-) capable of complexation with cations [3]. Surface charge is dependent upon the proton condition of the external milieu. The thermodynamic controls on charge buildup and metal binding at specific microbe-solution interfaces has been studied [4,5]. For example, the uptake of Cd^{2+} , Pb^{2+} , and Cu^{2+} onto the cell wall of *B. subtilis* was greatest in a proton deficient environment (pH 6-9) with the carboxyl and phosphate groups implicated as the major sorption

sites [4]. Alteration of the carboxyl groups of *B. subtilis* severely limited cation (Na, K, Mg, Ca, Mn, Fe³⁺, Ni, Cu, and Au³⁺) deposition [6]. At pH 4.0, Ag⁺ was efficiently removed (89%) from solution and found as discrete colloidal aggregates at the cell surface and in the cytoplasm; La³⁺ formed needle-like precipitates at the cell surface [7]. In addition to surface sorption of cations (biosorption), transport of cations across the cell membrane and accumulation within the cell (bioaccumulation) is another mechanism for the formation of biocolloids [8].

The halophilic bacteria normally found at the WIPP site require 20-25% w/v dissolved salts for growth and metabolism. These extremophiles thrive in an environment that imparts a severe osmotic stress on the cell. Many halophiles transport cations, specifically K⁺, across the cell membrane and into the cells in order to counter the osmotic stress of their environment [9]. There is little information on biosorption and bioaccumulation of actinides by extreme halophiles. Here we report the biosorption and bioaccumulation of uranium by a halophilic bacterium (WIPP 1A) isolated from the WIPP site.

EXPERIMENT

Bacterial Culture

The halophilic bacterial culture (WIPP 1A) was isolated from sediment slurry from the WIPP surficial environment [1]. The bacterium was grown in medium containing the following (g/l): sodium succinate, 5; KNO₃, 1; KH₂PO₄, 0.25; yeast extract (Difco), 0.5, WIPP salt (primarily halite), 200; and deionized water to 1000 ml. The pH was adjusted to 6.8. The culture was grown under anaerobic (denitrifying) conditions, using nitrate as the electron acceptor at 30 ± 2°C for 48 hours. This culture is a gram-positive rod that will not grow in medium containing less than 18% w/v dissolved salts; it produces the carotenoid α -bacterioruberin characteristic of archaeobacterial halophiles [10], and does not reduce uranium or iron under anaerobic conditions nor use them as electron acceptors.

Preparation of Bacterial Cells

The cells were harvested by centrifugation of a 48-h old culture at 5000 x g for 15 min. [11]. The cell pellet was washed twice with filter sterilized (0.2 μ m) 20% w/v NaCl electrolyte adjusted to pH 5.0. The pellet was resuspended in 40 ml of the electrolyte to an optical density of 0.8 (measured at 600 nm). A 1.0 ml subsample was preserved in 5% v/v formalin for cell counts by direct microscopy using DAPI staining and epifluorescence microscopy [12]. Cell dry weights were obtained by washing with ammonium formate to displace dissolved salts and drying at 90 ± 2°C overnight.

Cell Surface Charge Determination

The cell suspension (40 ml) was adjusted to pH 4.0 with 0.1N HCl in a glass titration vessel and fitted onto the titration head of a Mettler DL-53 autotitrator fitted with a Mettler DG111 pH electrode. Nitrogen gas was continuously purged into the headspace of the titration vessel to exclude air. Cells were titrated from pH 4 to ~10 with 0.001N NaOH (Fisher Certified). Titrations proceeded in dynamic mode with titrant added (0.02 to 0.2 ml mV⁻¹) upon establishment of equilibrium conditions (dE/dt) which were defined as ≤ 0.1 mV s⁻¹. Cell-free electrolyte (after exposure to cells for 1-hour followed by centrifugation and filtration) was titrated as a blank and subtracted from data for cell titrations. Separate experiments were run to

DISCLAIMER

This report was prepared as an account of work sponsored by an agency of the United States Government. Neither the United States Government nor any agency thereof, nor any of their employees, make any warranty, express or implied, or assumes any legal liability or responsibility for the accuracy, completeness, or usefulness of any information, apparatus, product, or process disclosed, or represents that its use would not infringe privately owned rights. Reference herein to any specific commercial product, process, or service by trade name, trademark, manufacturer, or otherwise does not necessarily constitute or imply its endorsement, recommendation, or favoring by the United States Government or any agency thereof. The views and opinions of authors expressed herein do not necessarily state or reflect those of the United States Government or any agency thereof.

DISCLAIMER

Portions of this document may be illegible in electronic image products. Images are produced from the best available original document.

assess the reversibility of surface charging and to specifically examine the origins of any titration hysteresis.

Titration Data Analysis

FITEQL 3.0 [13] was used to resolve potentiometric titrations into likely reaction stoichiometries and surface acidity constants. In the application of interest, FITEQL takes as input sequential data, including the amount of base added to achieve a stable pH, and the extent of dilution caused by the titrant addition. A constant capacitance model was used to fit surface charge data [14]. We used FITEQL's default analytical errors; relative errors of 0.01 units for pH and 0.02303 for $[H^+]$. The data was manually fit to 2-site models. Initial scoping work showed that each of the titration curves could be roughly fit using the same two pKs; $pK_1 = 5.7$ and $pK_2 = 8.7$. Therefore, the approach was to fix the two site pKs and iterate for site densities which provide a good fit to the data.

Actinide Biosorption

Uranyl ion uptake by WIPP 1A was examined in 4M NaCl at pH 5, 7, and 9. Cells were prepared as described for titration except that they were diluted to an optical density of 0.6 ($\sim 1 \times 10^8$ cells/ml) and pre-equilibrated at pH 5, 7 or 9 for 1 hour. Uranyl nitrate (BDH Chemicals Ltd., UK), 1:1 uranium:citrate, or 1:10 uranium:carbonate (pH 9 only) was added to obtain a final concentration of 0.125 mM and the pH was controlled using a Mettler DL-53 autotitrator over a 1-hour contact time. Solutions were filtered through a 0.2 μ m nylon syringe and the amount of uranium retained on the filter (minus the control) was reported as biomass associated. Uranium was analyzed using a Liberty 150 inductively-coupled plasma atomic emission spectrometer (Varian Corp.).

Transmission Electron Microscopy (TEM) and Energy Dispersive X-ray Spectroscopy (EDS)

The location of uranium deposition on the cell surface or inside the bacterial cells was determined by TEM and EDS. After exposure to uranium, the bacterial cells were preserved in 1% v/v EM-grade glutaraldehyde (Polysciences, Inc.) in 4M NaCl, pH 5.0. Whole cell mounts were prepared to confirm the presence of U with the bacteria. In order to locate the areas of deposition the cells were embedded in plastic without adding osmium or uranyl acetate and thin sectioned for TEM. A Philips EM400 TEM, operating at 100kV, with a Link Analytical Ltd. x-ray spectrometer was used to examine the thin sections to determine sites of uranium deposition.

Extended X-ray Absorption Fine Structure (EXAFS)

Resting cells of WIPP 1A were exposed to uranium (0.125 mM) at pH 5, as previously described. The cells were transferred without further treatment to a heat sealed polypropylene bag and analyzed at the X18B beamline at the National Synchrotron Light Source using the U L_{III} absorption edge (17.166 keV) with fluorescence detection. Uranyl chloride, uranyl formate, uranyl acetate, and uranyl succinate were obtained from Atomergic Chemical (NY); uranyl hydroxide, uranyl phosphate, uranyl succinate, and uranyl citrate were prepared from uranyl nitrate. Standards were ground to a fine powder and diluted (10%) in boron nitride before transfer to polypropylene bags. Multiple scans (3 to 12 depending on signal to noise ratio) were collected for each sample and averaged. Fourier transformed EXAFS spectra, a pseudo-radial distribution function (PRDF) representing the radial coordination shells of the near-neighbor

atoms surrounding the uranium, were obtained using a multi-step data analysis process which included background subtraction and normalization to the edge-jump height followed by Fourier transformation of the k^3X -weighted spectra. Distances were not corrected for actual peak positions and are displaced toward shorter distances due to atom pair phase shifts ($\Delta R \approx 0.3-0.5$ Å) which differ for each neighboring atom.

RESULTS

The solubility of uranyl nitrate decreased with increasing pH (Table 1). Uranyl nitrate was removed from solution by WIPP-1A cells, with the greatest amount at pH 5 (32%) and decreased with an increase in pH. Uranium complexed with citric acid was soluble at all pHs tested, however there was little uptake by the cells except at pH 9 (14%) which may be attributed to dissociation of the complex at higher pH. Uranyl EDTA was not soluble at any pH and therefore was not bioavailable. Uranyl carbonate species was stable in solution only at higher pH (> 7) but was not removed by the cells at pH 9. The lack of removal of uranyl citrate and uranyl carbonate complex by the bacterium was due its neutral (UO_2CO_3) or negative charge ($UO_2(cit)_2^{2-}$, $UO_2(CO_3)_2^{2-}$, $UO_2(CO_3)_3^{4-}$).

Table 1. Biosorption of uranium by WIPP 1A Isolate

Form of uranium added	pH	Uranium in Solution*	Uranium associated with cells
		mM	(%)
Uranyl nitrate	5	0.121	32±1
	7	0.039	21±3
	9	0.008	13±1
Uranyl citrate	5	0.125	<1
	7	0.125	<1
	9	0.125	14
Uranyl EDTA	5	<0.001	----
	7	<0.001	----
	9	<0.001	----
Uranyl carbonate	9	0.125	<1

*Concentration of uranium added was 0.125 mM.

---- = not determined

The titration curve for WIPP 1A and the FITEQL fit is shown in Figure 1A. The number of negatively charged sites increased with pH. The titration curve was fit to two pKs: 5.7 and 8.7. The pK's for simple carboxylic acids fall between 4 and 6, and the pK's of hydroxo groups fall between 9 and 11. The deprotonation constant of $H_2PO_4^-$ is 7.2; based on this the phosphate group was ruled out as a major functional group for actinide sorption by the bacteria. Figure 1B shows the speciation for the carboxyl and hydroxyl groups at the WIPP 1A bacterial cell surface based upon the model calculations.

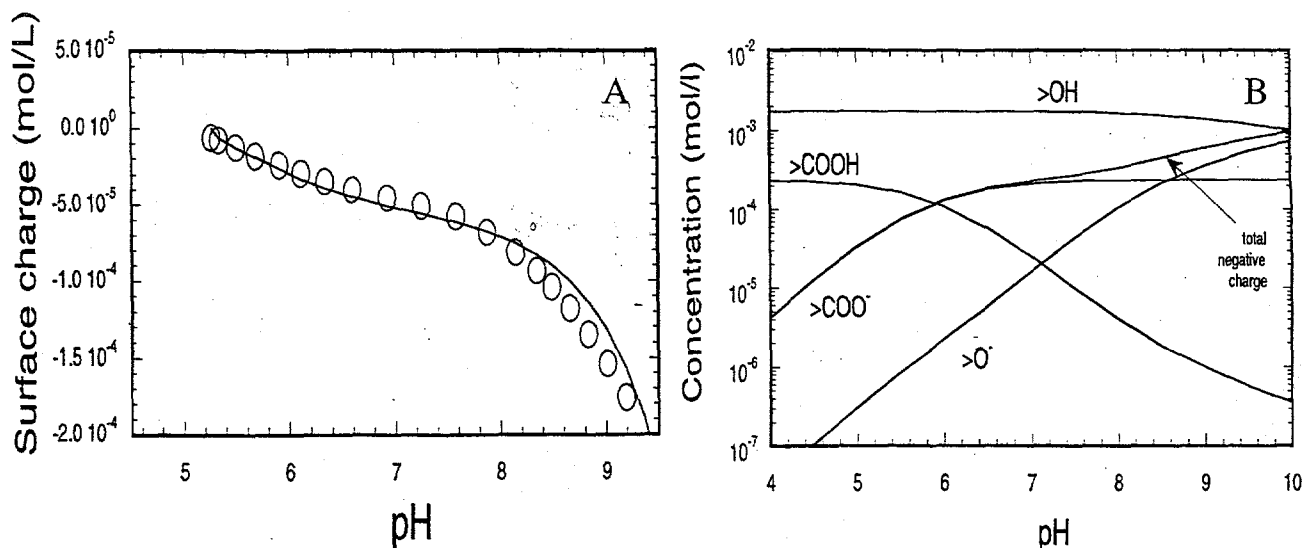


Figure 1. (A) Titration of WIPP 1A cells; open circles are data, smooth line is FITEQL fit, (B) Speciation of cell-surface functional groups as a function of pH.

Figure 2 shows Transmission Electron Microscopy (TEM) of thin-sections of WIPP 1A in 4M NaCl (A) without added uranium and (B) complementary Energy Dispersive X-ray Spectroscopy (EDS) spectra. In cells exposed to uranyl nitrate at pH 5, (Figure 2C) uranium is shown as electron-dense intracellular granules and also bound to the cell surface (areas of high contrast). In Figure 2D the EDS spectra of the intracellular granules shows them to be rich in uranium. The oxygen (O), phosphorus (P), sulfur (S), calcium (Ca), and iron (Fe) lines of the spectrum are naturally present in the cells due to the conditions they were grown under. The high copper (Cu) lines are from the copper EM grid used to support the specimen.

In addition to surface sorption at pH 5, uranyl ion was transported into the cell. This phenomenon was clearly elucidated by TEM and EDS. The TEM analysis shows that uranium was accumulated in the periplasmic space, as platy U precipitates, between the outer and plasma membranes; this imparted contrast to the cell wall due to the electron dense regions. In addition, uranium was packaged into discrete granules within the cytoplasm. The EDS analysis confirmed the presence of uranium in the granules, which appeared to be enriched in uranium due to its predominance in the granules. Control cells not exposed to uranium did not show any evidence of electron dense regions or intracellular granule formation. Intracellular uranium accumulation has been reported previously, but uranium existed as a fine-grained, platy precipitate [8]. Studies are in progress to determine the characteristics and the fate of the intracellular granular uranium.

Figure 3A compares the chi-weighted EXAFS spectra at the uranium L_{III} absorption edge of the uranium exposed cells with the uranium standards. The standards were chosen to determine the possible forms of uranium association with the cells including mono- (formate), bi- (acetate, succinate, oxalate), and tridentate (citrate) coordination of cell wall bound carboxylate groups as well as phosphate and hydroxyl bound uranium. Analysis of the $k^3(X)$ -weighted data shows distinct amplitude and phase shifts for each standard which is dependent upon nearest-neighbor atom association with uranium and therefore is diagnostic for each uranium-ligand association. Comparison of the amplitudes and phase shifts of the standards with the cell bound uranium does not lead to a positive identification of uranium speciation for the cells. However, it is noteworthy that uranium association with chloride in the cells is not indicated due to the absence of the diagnostic feature at 6.5 \AA^{-1} present for uranyl chloride.

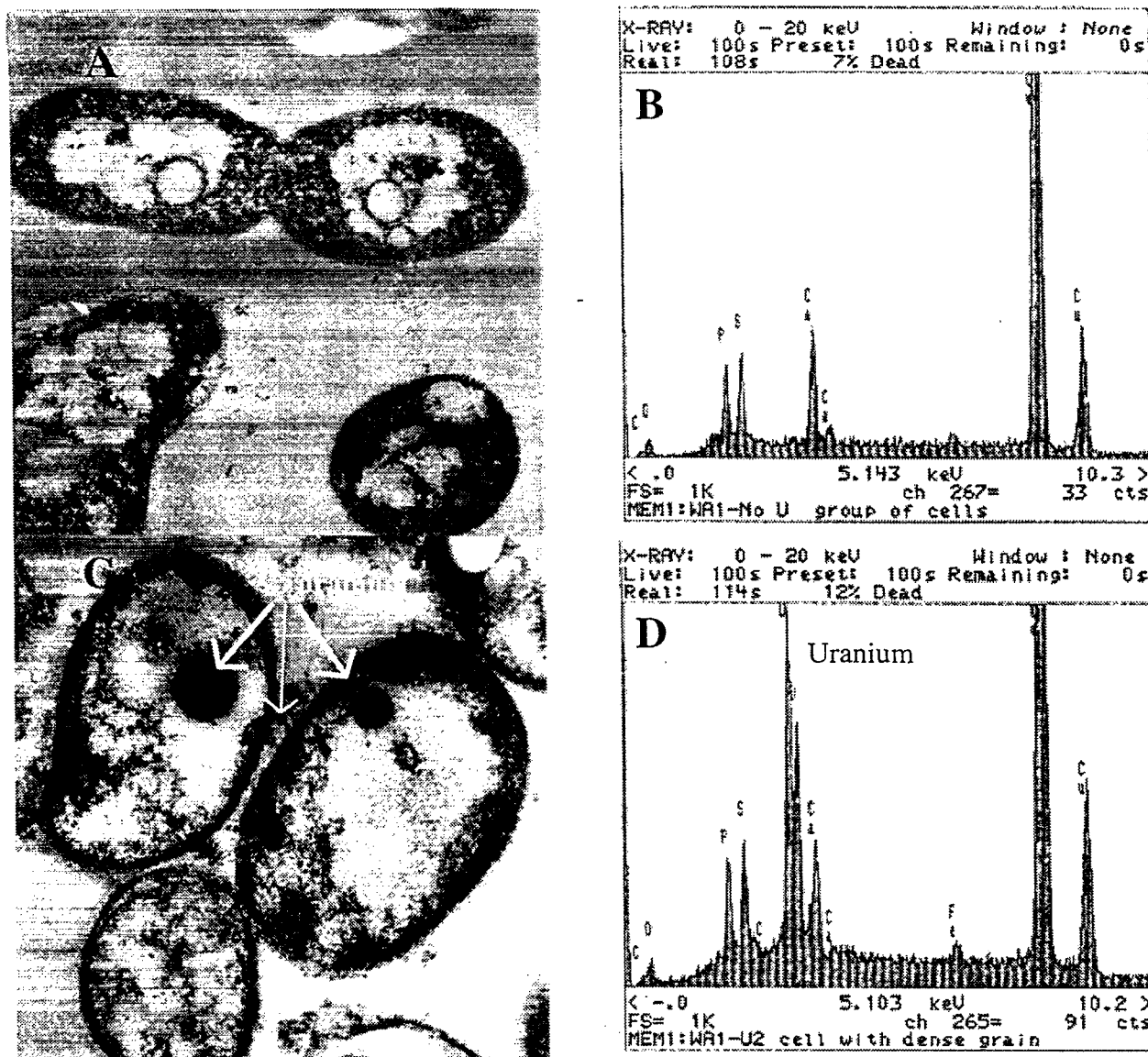


Figure 2. Biosorption and bioprecipitation of uranium as determined by TEM and EDS.

Figure 3B shows the Fourier-transformed (FT) data for the uranium standards. EXAFS probes the structural environment surrounding U up to several Å and any changes in spectral shape can be attributed to differences in the nearest neighbor atom including coordination number, average atomic distance, and atom type. The radial distribution of neighboring atoms is indicated by the location of the peaks. The first shell at 1.4 Å is due to scattering from the two axial oxygens closest to uranium, and the second shell at approximately 1.8-1.9 Å is a result of contributions from the axial oxygens of uranium which is usually five- or six-coordinate. Pronounced differences in the spectra are indicated by comparison of the height and positions of the second shells of each standard. For example, uranyl hydroxide has a small peak associated with the second shell which can be attributed to the large structural disorder in axial oxygens in the amorphous oxide. In contrast, uranyl chloride has a large magnitude peak associated with the second shell indicating a more structurally symmetrical association of atoms. Beyond the second shell contributions from other atoms in the compound including chloride, carbon, and oxygen are

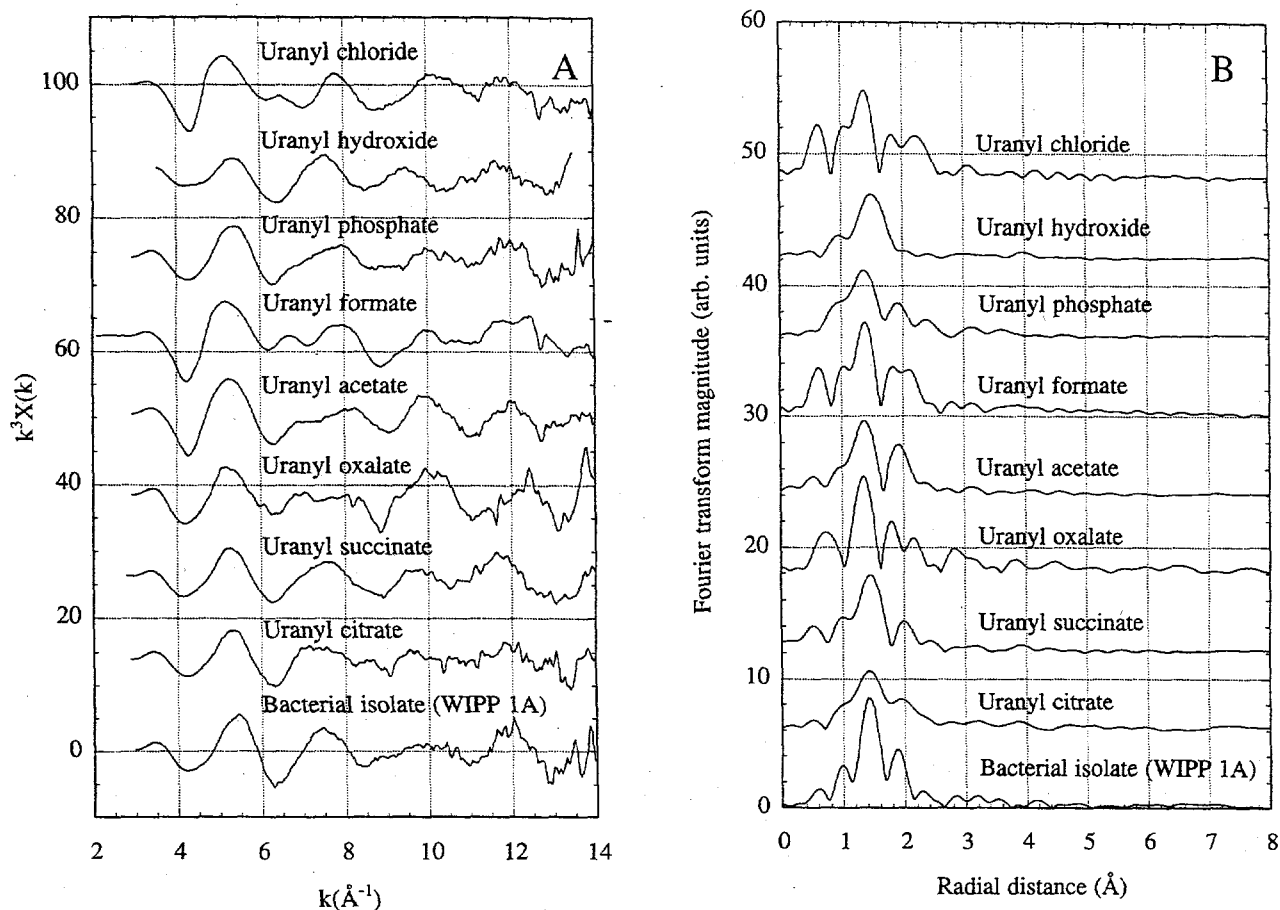


Figure 3. Extended x-ray absorption fine structure (EXAFS) analysis of uranium standards and WIPP 1A bacterial cells after exposure to uranium: (A) Chi-weighted and (B) Fourier-transformed data.

found. The presence of these atoms however are usually difficult to detect due to multiple scattering effects as well as weak spectral contributions from the low atomic number atoms. As with the chi data, it is difficult to make a comparison of the uranium in the cells and the standards. The lack of positive identification in the EXAFS is due to the fact that it is a bulk technique. More than one association of uranium will be averaged depending on its concentration in the sample. The presence of uranium on the cell wall as well as inside the cell as shown by TEM confirms this finding.

CONCLUSIONS

- Uranium uptake by the WIPP repository-relevant extremely halophilic bacterium WIPP 1A was dependent upon uranium speciation. At pH 5, uranyl nitrate was bioavailable for both surface adsorption and intracellular accumulation while at higher pHs (7 and 9), uranium is only slightly soluble. The soluble species, uranium citrate and carbonate, do not interact with the bacterial cells. We have found in a separate study that the growth of WIPP 1A produces carbon dioxide which solubilizes uranium forming uranyl carbonate which is neither biosorbed nor bioaccumulated [15]. Uranium EDTA was not soluble at any pH, and therefore was not bioavailable.

- The carboxylate groups at the bacterial cell surface of WIPP 1A are the most likely functional groups available for interaction with bioavailable actinides. Titration data also suggest that the phosphate group is not a significant contributor to surface sorption in the bacterial species studied. At pH 5, positively-charged uranyl ion interacts with the deprotonated carboxyl groups. At pH 7 and 9, both the carboxyl and hydroxyl groups at the cell surface are deprotonated; however uranium is not bioavailable due to its predominance as neutral or negatively charged species (citrate or carbonate) at high pH.
- In addition to surface sorption, uranyl nitrate was transported inside the cell. The bacterial cells that accumulated uranium as granules are clear examples of actinide-biocolloids. Their chemical composition, transport characteristics, and persistence are not known.
- EXAFS analysis of the WIPP 1A bacterial cells after exposure to uranium confirms the presence of two or more unidentified uranium phases associated with the cells. The nature of the association of uranium with the cells requires further examination.

ACKNOWLEDGEMENTS

This work is supported by Sandia National Laboratories. The authors thank Susan Raevsky and Michelle Gaston for their skillful assistance.

REFERENCES

1. A.J. Francis, J.B. Gillow, and M.R. Giles. Microbial gas generation under expected Waste Isolation Pilot Plant repository conditions. SAND96-2582 (1997).
2. A.J. Francis, J.B. Gillow, C.J. Dodge, M. Dunn, K. Mantione, B.A. Strietelmeier, M.E. Pansoy-Hjelvik, and H.W. Papenguth, *Radiochim. Acta* (in press).
3. T.J. Beveridge. *Can. J. Microbiol.* **34**, 363 (1988).
4. Daughney C. J. and Fein J. B. *J. Coll. Interf. Science* **198**, 53 (1998).
5. Fein J. B., Daughney C. J., Yee N., and Davis T. *Geochim. Cosmochim. Acta* **61**, 3319 (1997).
6. T.J. Beveridge and R.G.E. Murray. *J. Bact.* **141**, 876 (1980).
7. M.D. Mullen, D.C. Wolf, F.G. Ferris, T.J. Beveridge, C.A. Flemming, and G.W. Bailey. *Appl. Environ. Microbiol.* **55**, 3143 (1989).
8. S. Krueger, G.J. Olson, D. Johnsonbaugh and T.J. Beveridge. *Appl. Environ. Microbiol.* **59**, 4056 (1993).
9. L.N. Csonka. *Microbiol. Reviews* **53**, 121 (1989).
10. A. Oren, in *The Biology of Halophilic Bacteria*, edited by R.H. Vreeland and L.I. Hochstein (CRC Press, Boca Raton, 1992), p. 35.
11. G.D. Sprott, S.F. Koval, and C.A. Schnaitman, in *Methods for General and Molecular Bacteriology*, edited by P. Gerhardt (American Society for Microbiology Press, Washington D.C., 1994), p. 72.
12. R.L. Kepner Jr. and J.R. Pratt, *Microbiol. Rev.* **58**, 603 (1994).
13. A.L. Herbelin and J.C. Westall J. C., FITEQL - A computer program for determination of chemical equilibrium constants from experimental data. Dept. Chemistry, Oregon State Univ. (1994).
14. J.B. Gillow, A.J. Francis, H.W. Papenguth, and P.V. Brady, (in preparation).
15. A.J. Francis, C.J. Dodge, J.B. Gillow, and H.W. Papenguth, (in preparation).